This article was downloaded by:
On: *14 January 2011*
Access details: *Access Details: Free Access*
Publisher *Taylor & Francis*
Informa Ltd Registered in England and Wales Registered Number: 1072954 Registered office: Mortimer House, 37-41 Mortimer Street, London W1T 3JH, UK

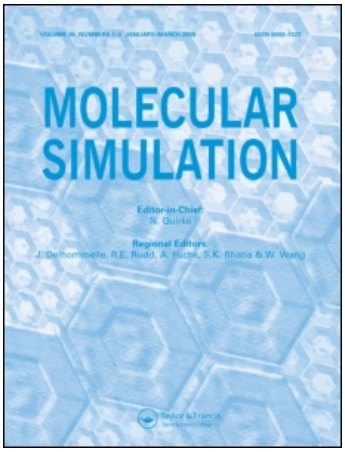

Molecular Simulation
Publication details, including instructions for authors and subscription information:
http://www.informaworld.com/smpp/title~content=t713644482

The Adsorption of Argon and Nitrogen in Silicalite-1 Zeolite: A Grand Canonical Monte-Carlo study

Dominique Douguet[a]; Roland J. -M. Pellenq[a]; Anne Boutin[a]; Alain H. Fuchs[a]; David Nicholson[b]
[a] Laboratoire de Chimie-Physique des Matériaux Amorphes, btiment 490, URA-CNRS 1104, Université de Paris-Sud, Orsay, France [b] Imperial College of Science, Technology and Medicine, London, United Kingdom

To cite this Article Douguet, Dominique , Pellenq, Roland J. -M. , Boutin, Anne , Fuchs, Alain H. and Nicholson, David(1996) 'The Adsorption of Argon and Nitrogen in Silicalite-1 Zeolite: A Grand Canonical Monte-Carlo study', Molecular Simulation, 17: 4, 255 — 288
To link to this Article: DOI: 10.1080/08927029608024112
URL: http://dx.doi.org/10.1080/08927029608024112

PLEASE SCROLL DOWN FOR ARTICLE

Full terms and conditions of use: http://www.informaworld.com/terms-and-conditions-of-access.pdf

This article may be used for research, teaching and private study purposes. Any substantial or systematic reproduction, re-distribution, re-selling, loan or sub-licensing, systematic supply or distribution in any form to anyone is expressly forbidden.

The publisher does not give any warranty express or implied or make any representation that the contents will be complete or accurate or up to date. The accuracy of any instructions, formulae and drug doses should be independently verified with primary sources. The publisher shall not be liable for any loss, actions, claims, proceedings, demand or costs or damages whatsoever or howsoever caused arising directly or indirectly in connection with or arising out of the use of this material.

Molecular Simulation, 1996, Vol. 17, pp. 255–288
Reprints available directly from the publisher
Photocopying permitted by license only

© 1996 OPA (Overseas Publishers Association)
Amsterdam B.V. Published in The Netherlands under
license by Gordon and Breach Science Publishers SA
Printed in Malaysia

THE ADSORPTION OF ARGON AND NITROGEN IN SILICALITE-1 ZEOLITE: A GRAND CANONICAL MONTE-CARLO STUDY

DOMINIQUE DOUGUET[1], ROLAND J-M PELLENQ[1,*], ANNE BOUTIN[1], ALAIN H. FUCHS[1] and DAVID NICHOLSON[2]

[1]*Laboratoire de Chimie-Physique des Matériaux Amorphes, bâtiment 490, URA-CNRS 1104, Université de Paris-Sud, 91405 Orsay, cédex, France*
[2]*Imperial College of Science, Technology and Medicine, 2AY SW7, London, United Kingdom*

(Received January 1996; accepted February 1996)

Downloaded At: 19:17 14 January 2011

Grand Ensemble Monte-Carlo simulations of adsorption of argon and nitrogen in silicalite have been performed using a new adsorbate/zeolite potential function. In both cases, a good agreement with zero coverage data (Henry law constant and isosteric heat of adsorption) has been obtained. For argon, the simulated isotherm at 77 K exhibits the experimentally observed step. This is attributed to an in site/off-site phase transition of the adsorbed phase. The calculated neutron diffraction spectra are in reasonable agreement with those obtained experimentally. Furthermore, we suggest, in light of recent ^{40}Ar diffraction experiments of Tosi-Pellenq and Coulomb [18,44], that the shift in pressure between the simulated and the experimental isotherms corresponds to changes in the zeolite structure accompanied with the adsorbate phase transition itself. For nitrogen, only the first of the two experimentally observed steps is reproduced in the simulation. This step corresponds to an ordering of the adsorbed phase. The fact that the second step is missing in the simulated isotherm supports the hypothesis of a distortion of the zeolite framework under the stress of the adsorbed fluid at high loading.

Keywords: Argon; nitrogen; silicalite; Grand Canonical Monte-Carlo

1. INTRODUCTION

Zeolites are crystalline microporous aluminosilicates (or aluminophosphates) which form the basis of many industrial processes in gas separation

*To whom correspondence should be sent Present address: Centre de Recherches sur la Matière Divisée, UMR-CNRS 131, 1b rue de la Férollerie, 45071 Orléans cédex 02, France.

or in (heterogeneous) catalysis. At a fundamental level, the thermodynamic properties of confined fluids in porous materials are adequately described by the theory only in the case of model mesoporous materials such as slit pores or cylinders [1]. Until quite recently, the thermodynamic theory of adsorption in mesoporous materials relied mainly on the Kelvin equation which has an intrinsic limitation when one considers micropores (widths or diameters less than 20 Å). However, this theory correctly predicts the (first order) transition pressure of the capillary condensation for a wetting fluid (*i.e.* the pressure at which the mesopore fills with a dense, liquid-like phase of the adsorbate). It is important to mention the recent theoretical advances based on a density functional formalism [2, 3]. This theory covers both the microporous and the mesoporous ranges. For instance, this new theory predicts, in agreement with experiments [4], and simulation work [5], the progressive vanishing of the capillary condensation phenomenon as the pore size decreases towards the microporous range. However, since the atomic details of the solid surface and the adsorbate-adsorbate interaction are not explicitly taken into account, density functional theory cannot quantitatively reproduce the equation of state (namely the adsorption isotherm) of a confined molecular fluid in a micropore. For example the adsorption isotherm of xenon in zeolite A, obtained from density functional theory, seriously underestimates the amount adsorbed at high-pressure [6].

Simulation techniques (Monte-Carlo or Molecular Dynamics methods) are now considered as a third way between theory and experiment, in the study of physical phenomena at a molecular level. These methods have been extensively applied in the field of gas adsorption over the last fifteen years. They are based (i) on an accurate description of the intermolecular potential functions between the adsorbate molecules and the solid surface and between the adsorbate molecules themselves and (ii) on time or statistical ensemble averages from which one can extract thermodynamic (usually equilibrium) data to be compared with experiment [7]. Transport and adsorption properties of a given fluid confined in a microporous cavity at low temperature, are entirely dictated by the location, shape and depth of adsorption sites (which closely depend on the chemical nature and the spatial distribution of the atoms in the substrate). It is thus clear that molecular simulation techniques have an advantage over available theories in describing and predicting properties of such interfacial systems.

From an experimental point of view, the procedure for the thermodynamic characterization of porous materials is based on the measurement of adsorption isotherms of argon or nitrogen at low temperature (usually 77 K). One

Downloaded At: 19:17 14 January 2011

can extract from these adsorption isotherms important data such as the pore-size distribution which gives the most probable diameter (or width) for a porous material containing various types of porosity (for instance porous carbons). Silicalite-1 zeolite is a pure siliceous form of MFI (or ZSM-5) crystals. It contains two types of intercrossing microporous channels, namely the straight and the zig-zag channels, whose apertures are both about 5 Å across [8]. This crystal can undergo a structural (ferroelastic) phase transition from a low temperature monoclinic form to a high temperature orthorhombic structure [8]. This phase transition is temperature-controlled (it occurs at 340 K for the unloaded crystal) and can also be induced at lower temperature by the presence of aromatic molecules in the pores [8, 46]. The argon and nitrogen adsorption isotherms at 77 K have been measured by several research groups: surprisingly, the argon and nitrogen adsorption isotherms both exhibit steps (one for argon [10, 11, 15, 16, 17], two for nitrogen [10, 11, 12, 13, 14, 16, 19]) which were attributed to phase transitions of the adsorbed phases. These transitions cannot be first order capillary condensations since the silicalite inner cavity diameters are well into the microporous domain. In the case of argon, the single step was interpreted by Llewellyn *et al.* [17], on the basis of microcalorimetry and neutron diffraction experiments, as a transition from a "liquid-like phase" to a "crystalline phase". Upon desorption, the argon adsorption isotherm exhibits hysteresis [18]. For nitrogen, the same authors [19] claimed that the first transition corresponds to a transition from a "disordered liquid phase" to a "lattice fluid-like phase" and that the second transition corresponds to a transition from a "lattice fluid-like phase" to a "crystalline-like solid phase". It is interesting to note that the first transition which occurs at quite low relative pressure ($2 \cdot 10^{-3}$ P/P_0) has not been found by many research groups probably because it is more visible on a calorimetric curve [19] (giving the differential enthalpy or the isosteric heat of adsorption as a function of coverage) than on the adsorption isotherm; it corresponds to a small step on the isotherm (about 2 nitrogen molecules per unit cell *i.e.* an increase of 6.5% with respect to the total amount adsorbed) while the second transition corresponds to a step of 7 nitrogen molecules per unit cell *i.e.* an increase of 22.7% with respect to the total amount adsorbed (31 N_2 per unit cell). Upon desorption, the adsorption isotherm also exhibits an hysteresis loop for the second step [10, 11, 12]. Very recently, some authors have studied the second phase transition for nitrogen by means of ^{15}N NMR technique [20, 21]. They have found that the isotherm step does not correspond to a liquid to solid transition, since at 77 K both NMR signals (before and after the transition) are signatures of

Downloaded At: 19:17 14 January 2011

fluid phases. A solid nitrogen phase is reached at both loadings when the temperature is decreased down to 11 K. The same authors concluded that, under the confinement effect in zeolitic micropores, the temperature of the liquid to solid transition for nitrogen was shifted 50 K lower than the normal transition temperature. They also claimed that the high loading nitrogen phase was in fact made of two different phases coexisting simultaneously (on the NMR time scale) in two different regions inside the microporous zeolitic network: a liquid-like phase and a confined fluid with restricted motion. As the temperature is lowered, the change from a liquid-like to a broader signal (reflecting the more restricted environment) is progressive in contrast to standard temperature dependent phase transition. The same conclusion was drawn when the pressure was increased at constant temperature. However, this ^{15}N NMR study does not provide any mechanism to explain the (sudden) adsorption step and hysteresis. Future ^{15}N NMR works should concentrate on the measurements of T_1 and T_2 as the magnetic field frequency and the adsorbate concentration vary. As far as argon is concerned, Conner *et al.* [9] concluded that this adsorbate does not solidify in the pores of silicalite at 77 K: "*there is no compelling reason to conclude that argon would solidify within 6 K of its normal melting point since nitrogen adsorbed in silicalite does not become a solid below 11 K (a freezing point depression of 50 K)*". The origins of the steps and hysteresis present in the adsorption isotherms of argon and nitrogen in silicalite at low temperature are therefore not clear and the interpretations even contradictory in the particular case of nitrogen. The remainder of the paper is organized as it follows. Section 2 is devoted to the intermolecular potential functions used to describe the adsorbate/adsorbate and adsorbate/zeolite interactions. The Grand Canonical Monte-Carlo technique is outlined in Section 3. Results are presented and discussed in Section 4.

Downloaded At: 19:17 14 January 2011

2. POTENTIAL FUNCTIONS USED IN THE GCMC SIMULATION

2.1. Adsorbate/Zeolite Potential Function

The adsorbate-zeolite potential function used in this work is based on the usual partition of the total interaction energy. The total potential function considers the interactions between each atom of the adsorbate molecule with each zeolite species. The general expression for the adsorbate-zeolite potential function is given by [22]:

$$U^{\text{total}} = U^{\text{coul}} + U^{\text{ind}} + U^{\text{disp}} + U^{\text{rep}} \tag{1}$$

Analytical expressions for the coulombic, the induction and the dispersion terms are derived from the perturbation theory applied to intermolecular interactions. The nitrogen/zeolite potential function contains an electrostatic term which acts at long range since nitrogen has a permanent quadrupole interacting with the partial charge of the silicalite crystal ($-1e$ and $+2e$ for oxygen and silicon respectively [23]). The analytical formulation of the interaction depends on the model used to reproduce the nitrogen quadrupole. For example, the coulombic interaction between the nitrogen quadrupole and each zeolite atom can be represented by a point quadrupole which has a magnitude Θ, placed at the centre of mass of the molecule interacting with the partial charge q placed on the crystallographic site of the zeolite species. The full multipole expansion for a linear molecule interacting with a point charge is given by Buckingham [22]. According to the multipole expansion used in the perturbation theory, the above expression is valid at long range, *i.e.* for distances much larger than the sum of van der Waals radii. A better treatment of electrostatic interactions can be achieved using Distributed Multipole Analysis [24]. A simpler alternative is to consider the nitrogen molecule as a set of charges positioned to reproduce the magnitude of the quadrupole according to the following expression:

$$\Theta = \sum_{i}^{n} q_i r_i^2 \tag{2}$$

where n is the number of charges used to mimic the quadrupole ($\Theta = -0.9924$ au). A four charge model for nitrogen has been proposed from a fit to the *ab initio* potential surface [25]. This model accurately reproduces the properties of bulk nitrogen over a wide range of thermodynamic conditions and has been used to simulate nitrogen adsorption on graphite [26]. The quadrupole-charge interaction is determined by placing four point charges along the nitrogen molecular axis at the positions ± 0.847 Å and ± 1.044 Å with respect to the molecular mass centre. The interior and outer charges are $q = 0.373e$ and $-0.373e$ respectively. The nitrogen molecule is considered to be rigid. The fact that the model places positive charges between the atoms along the actual bond goes against chemical intuition which would lead one to expect a higher charge density in the bond. Other versions of the model exist based on three or five charge distributions [27]. The treatment of the nitrogen molecule within the frame of the DMA method places atomic dipoles directed towards the centre of the molecule to describe the lone pairs of electrons on the N atoms. In addition, there is a negative charge at the centre of the bond, balanced by

Downloaded At: 19:17 14 January 2011

positive charges on the atoms as expected on chemical grounds. In the case of the four charge model used in this work, the quadrupole-charge electrostatic interaction in the nitrogen/silicalite potential function is handled as a sum of charge-charge coulombic terms. This term is strictly pair additive. Since the partial charges carried by the nitrogen molecule are those reported in the description of the adsorbate-adsorbate intermolecular potential function, the description of the adsorbate/adsorbent coulombic interaction is fully consistent with the adsorbate-adsorbate potential function. The Ewald sums technique [27,40] is used in order to calculate the nitrogen/zeolite coulombic interaction in an appropriate manner (see below). The coulombic interaction for the Ar/silicalite system is obviously zero.

The induction energy is given by the first term of the induction multipole expansion:

$$U^{\text{ind}}(r_{ij}) = -\frac{1}{2}\alpha_i^A\{(E(r_{ij})\}^2 \tag{3}$$

Downloaded At: 19:17 14 January 2011

According to the reference system given for the coulombic interaction, α_i^A is the dipole polarizability of the atom i pertaining to the adsorbed molecule A and $\mathbf{E}(\mathbf{r})$ is the electrostatic field at the position occupied by the atom i due to the partial charges carried by the framework species. It can be shown that the induction energy derived from the perturbation theory for intermolecular interaction [22] is not pair-additive. Even for polar liquids such as water, this term contributes very little to the total interaction energy [28] so that the expression presented above is sufficient. Moreover, we consider that the adsorbed molecules in the pore do not polarize the framework atoms, so that there is no back-polarization effect. In the particular case of the nitrogen/silicalite system, the induction interaction is handled by considering a two centre molecule and is the sum of the product of the total electric field with the nitrogen atomic polarizability.

The third term of the general expression of the adsorbate-zeolite potential function corresponds to the dispersion energy. The dispersion energy is given by the following multipole expansion [34]:

$$U^{\text{disp}}(r_{ij}) = -f_6\frac{C_6^{ij}}{r_{ij}^6} - f_8\frac{C_8^{ij}}{r_{ij}^8} - f_{10}\frac{C_{10}^{ij}}{r_{ij}^{10}} - \cdots + \text{three body terms} \tag{4}$$

with

$$f_{2n} = 1 - \left[\sum_{k=0}^{2n}\frac{(b^{ij}r_{ij})^k}{k!}\right]\exp(-b^{ij}r_{ij}) \tag{5}$$

Pellenq and Nicholson have recently shown [29, 30] that the dispersion coefficients ($C_6^{ij}, C_8^{ij}, C_{10}^{ij}$...) can be all obtained from the knowledge of the dipole polarizability and an effective number of electron which is directly linked with the partial charge of each interacting species. The subscripts i and j have the same meaning as those used for the coulombic and the induction interactions. The f_{2n} functions ($n = 3, 4, 5$) are damping functions used to represent possible electronic exchange between the two species in interaction. Their effect is to attenuate the dispersion part of the potential function at small separations [34]. These functions are parametrized with the single repulsive parameter b^{ij} (see below) corresponding to each ij pair in interaction. The dispersion three-body terms mentioned in the last expression involve triplets of species, in which one atom pertains to the adsorbed molecules and the other two are zeolite species. It has been shown [29,30] that the three-body dispersion coefficients involved in the three-body dispersion terms can also be obtained from the dipole polarizability and the partial charge of each interacting species. Thus these two atomic parameters are crucial for the calculations of the coulombic, induction and dispersion terms. In the particular case of the nitrogen/silicalite system, the dispersion interaction is calculated by considering each nitrogen atom in the nitrogen molecule individually. Therefore, one has to find atomic parameters for the nitrogen atom taken from the molecular environment in terms of effective number of electrons and the dipole polarizability. Claverie *et al.* [31] have proposed a simple recipe to find atomic polarizability for atoms in a molecule from a knowledge of bond polarizability by considering the number of bonding electrons: it turned out that for the simple case of the nitrogen molecule, the atomic dipole polarizability is simply a half of the molecular polarizability. Thus the atomic nitrogen within the nitrogen molecule has a polarizability $\alpha_N = 5.93\ a_0{}^3 (0.88 \text{Å}^3)$. One can consider that the total partial charge at each nitrogen centre is zero since each atom in the molecule is neutral; the number of effective electrons to be used in the dispersion calculations is simply that of the free and isolated atom.

The last term in the expression of the total adsorbate-adsorbent interaction (equation 1) is the repulsive energy. This term represents the overlap between the wave functions of two interacting species at short range separations (Pauli principle). This term can be obtained in principle only from *ab initio* Hartree-Fock (SCF) calculations since it is not possible to derive any analytical expressions (as it is the case for the coulombic, induction and dispersion terms using the perturbation theory). As all other short range terms, the repulsive interaction is not pairwise additive. Unfortunately, the theory of intermolecular interaction has not been able to formulate any

Downloaded At: 19:17 14 January 2011

analytical expression for the three-body exchange-repulsion interactions. Thus, the two body expression used for the repulsive interaction in equation (1) is an approximate expression (see equation 6) which therefore has to be considered as an "effective repulsion term". This expression is only distance dependent. It has been shown [32] that a more accurate analytical representation for the repulsive interaction should be anisotropic *i.e.* should have an angle dependence in addition to the distance dependence found in the isotropic case. For the purpose of simulation, the repulsion interaction between two interacting species is usually represented by an exponential Born-Mayer term:

$$U^{rep}(r_{ij}) = A^{ij}\exp[-b^{ij}r_{ij}] \tag{6}$$

Thus, in the case of adsorption in silicalite zeolite, there is a pair of repulsive parameter (A and b) for each couple ij; the subscripts i and j describe the atoms of the adsorbate molecule and the zeolite species respectively. Böhm and Ahlrichs [33] have reported combination rules to estimate the repulsive parameters for a pair of hetero-atoms ij using those of the ii and jj pairs. We have chosen the second of the four Böhm and Alhrichs rules. This combination rule considers the following equations:

$$A^{ij} = \sqrt{A^{ii}A^{jj}} \tag{7}$$

and

$$b^{ij} = \frac{2b^{ii}b^{ij}}{b^{ii} + b^{jj}} \tag{8}$$

Thus, it is necessary to have estimates of the repulsive parameters for the pairs (O — O) and (Si — Si) as far as the zeolite atoms are concerned and the pairs (Ar — Ar) and (N — N) for the adsorbates considered in this study. The (Ar — Ar) and (N — N) repulsive parameters are obtained from references [34] and [33] respectively. The (Ar — O_{zeo}) and (Ar — Si_{zeo}) were adjusted in order to reproduce a large set of experimental zero coverage data (namely the isosteric heat and the Henry constant) over a range of temperature [29]. Reversing, the Böhm and Alhrichs rule, we have estimated the (O — O) and the (Si — Si) repulsive parameters: $A^{o-o} = 1543.5\ E_h, b^{o-o} = 2.19 a_0^{-1}$, $A^{Si-Si} 6163.4 = E_h$ and $b^{Si-Si} = 2.395\ a_0^{-1}$. Consequently, we have an estimate of the (N — O) and (N — Si) repulsive parameters. All coefficients for

Downloaded At: 19:17 14 January 2011

the dispersion and repulsion terms used for the total adsorption potential functions are given in Tables I and II for argon and nitrogen respectively.

For nitrogen, a grid was calculated for the repulsive, inductive and dispersive interactions in the same way as for the monatomic adsorbates over a portion of an orthorhombic unit cell embedded in a larger system

TABLE I Parameters in atomic units used in calculating the Ar-silicalite potential (in atomic units). 3-body coefficients are written as {XXX} with X = {D (dipole) or Q (quadrupole)}, see Reference [29]

	Ar-O	*Ar-Si*	*Ar-O-O*	*Ar-Si-O*
C_6	50.1	18.8		
C_8	966	261		
C_{10}	$2{\cdot}21.10^4$			
DDD			101	30.2
DDQ			325	71.8
DQD			325	97.2
QDD			450	135
DQQ			870	232
QDQ			$1.05{\cdot}10^3$	320
QQD			$1.05{\cdot}10^3$	434
QQQ			$4.68{\cdot}10^3$	$1{\cdot}03{\cdot}10^3$
$DDD_4(1)$			$-4.18{\cdot}10^3$	$-1.25{\cdot}10^3$
$DDD_4(2)$			$-3.05{\cdot}10^3$	-909
$DDD_4(3)$			$-3.05{\cdot}10^3$	271
A	711	1422		
b	2.045	2.09		

TABLE II Parameters in atomic units used in calculating the N_2-silicalite site-site potential (in atomic units). 3-body coefficients are written as {XXX} with X = {D (dipole) or Q (quadrupole)}, see Reference [29]

	N-O	*N-Si*	*N-O-O*	*N-Si-O*
C_6	26.69	9.965		
C_8	393.4	132.2		
C_{10}	771.9			
DDD			53.93	20.44
DDQ			198.9	38.88
DQD			198.9	76.92
QDD			155.0	58.66
DQQ			1210	119.9
QDQ			557.8	215.6
QQD			557.80	113.5
QQQ			3366	337.5
$DDD_4(1)$			-1193	-455.5
$DDD_4(2)$			-1629	-622.0
$DDD_4(3)$			-1629	-237.6
A	534.8	1069		
b	2.230	2.201		

Downloaded At: 19:17 14 January 2011

made of 27 unit cells (see reference [29, 35]). The grid was obtained by probing a portion of the unit cell (using crystal symmetry properties) with one atom of the diatomic molecule having all the properties of the atom in the molecule (in terms of atomic polarizability or atomic effective number of electrons). So that for each position of the molecular samass centre and for each orientation of the molecule with respect to a fixed frame (simulation box), the short range (repulsive, inductive and dispersive) energy was obtained by summing the interpolated energy for each atomic position calculated within a cut-off of 20 Å and therefore is the sum of two atomic contributions. The same grid technique was used for the electrostatic interaction: an electrostatic grid was calculated by probing the same portion of unit cell with a positive particle with a charge of $0.373e$ which is the magnitude of the charges used to model the quadrupole. The Ewald sum method was used in order to take account of the long range character of the coulombic interaction. This technique splits the calculations of the electrostatic interaction in two parts: a sum in direct space (within a cut-off of 20 Å in this work) and a sum in reciprocal space. The term in direct space can be written as (in atomic units) [27, 40]:

$$E_1 = q_i \sum_j \frac{q_j \operatorname{erfc}(\alpha r_{ij})}{r_{ij}} \tag{9}$$

where q_i and q_j are the probe and zeolitic atom charges respectively inside the 27 unit cell system and r_{ij} the separation between them, $\operatorname{erfc} = 1 - \operatorname{erf}$ with erf the error function. α is the Ewald parameter. The term in the reciprocal space can be written as (in atomic units):

$$E_2 = \frac{2\pi}{V} q_i \sum_{\vec{k} \neq 0} \sum_j q_j A(k) \cos(k \cdot r_{ij}) \tag{10}$$

with:

$$A(\mathbf{k}) = \frac{\exp\left(\frac{-k^2}{4\alpha^2}\right)}{k^2} \tag{11}$$

$\mathbf{k}$ is the reciprocal vector. It is written as:

$$\mathbf{k} = 2\pi\left(\frac{n_x}{A} + \frac{n_y}{B} + \frac{n_z}{C}\right) \quad \text{with} \quad \mathbf{k} \neq 0 \tag{12}$$

Downloaded At: 19:17 14 January 2011

where n_x, n_y, n_z are integers A, B, C the dimensions of the 27 unit cell box and V the volume ($V = ABC$). In addition, a third term, the so-called "self term" is given by:

$$E_3 = -\left[q_i^2 + \sum_j q_j^2\right]\alpha\pi^{-1/2} \tag{13}$$

Thus from a practical point of view, the Ewald sums technique requires two parameters: α and k^2_{max} (the maximum length of the reciprocal space vectors which defines the maximum number of reciprocal space vectors to be considered, $k^2_{max} = n_x^2 + n_y^2 + n_z^2$). α is a convergence parameter which has to be tuned in such a way that the direct space term E_1 converges within the cut-off distance (usually for a cubic box, α is taken equal to $5.6/L$ where L is the length of the box [27]). The number of reciprocal space vectors is chosen so that the reciprocal term E_2 reaches convergence (usually few hundred vectors of reciprocal space are needed). For the nitrogen/silicalite system, the optimum parameters are $\alpha = 0.279\ a_0^{-1}$ and $k^2_{max} = 108$. In order to avoid divergence at short separation during the coulombic grid calculation, the electrostatic energy in the direct space term was set to a large positive value when the distance between the probe charge and the framework species was less than 2 Å. Once the grid is calculated, the usual tridimensional grid-interpolation routine was used to obtain the total electrostatic energy of a nitrogen molecule in the simulation box. This energy is the sum of four terms; each term is the interpolated energy value at the position of one of the point charge on the molecule multiplied by ± 1 according to the quadrupole model presented above.

As for the rare gases/silicalite systems [29], we need to validate the nitrogen/ zeolite potential at zero coverage. One way to do so is to calculate thermodynamic properties at zero coverage such as the isosteric heat of adsorption and the Henry constant for different temperatures and compare them to available experimental data. The zero-coverage isosteric heat of adsorption at 77 K from the calculation is adjusted against its experimental value, measured via microcalorimetry at the same temperature ($q_{st} = 16.5$ kJ/mol [10, 11]). This fitting procedure is done by tuning the b^{O-N} starting from the value $b^{O-N} = 2.11\ a_0^{-1}$ first derived from the Böhm and Alhrichs combination rule. A value of $b^{O-N} = 2.23\ a_0^{-1}$ gives $q_{st} = 16.25$ kJ/mol at 77 K. We have further compared zero coverage simulated data with available experimental values at higher temperature. At 298 K, the calculated value for q_{st} is 16.45 kJ/mol^{-1} and compares well with the experimental values of 15.1 ± 1.3 kJ mol^{-1} [12] and 17.3 kJ/mol [36]. Figure 1 compares

Downloaded At: 19:17 14 January 2011

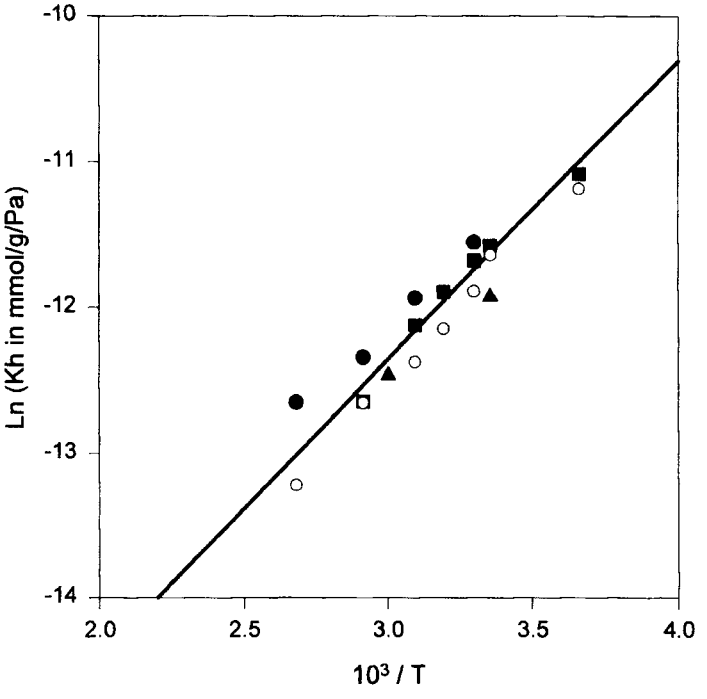

FIGURE 1 Henry law constants, experimental data (black circle) [36], experimental data (black square) [10], experimental data (black triangle) [50], (open circle) simulations (this work). The solid line is a linear regression through experimental data.

the calculated Henry law constants with several sets of experimental data [45] (at a given temperature, the Henry constant is simply the slope of the experimental adsorption isotherm in the low pressure region). The agreement between the calculated and the experimental thermodynamic quantities is good over a large range of temperature and confirms that the nitrogen/zeolite potential function gives a reasonable representation of the interactions between one nitrogen molecule and zeolitic species. Furthermore, we note that the potential model presented in this work for nitrogen adsorption in silicalite is primarily based on transferability principles from one adsorbate to another [29] and also from a zeolite structure to another [37,38]. However, the adjustment of a single parameter (the b^{O-N} repulsive parameter) in the validation procedure described above, indicates some shortcomings in the nitrogen/zeolite potential model which may be due to the (isotropic) description of the repulsive interaction and/or the use of partial charge distributions (for the nitrogen molecule itself and the zeolite structure).

Downloaded At: 19:17 14 January 2011

2.2. The Adsorbate/Adsorbate Potential Function

The argon-argon interactions were modeled by a 12–6 function using standard parameters for ε and σ (120 K, 3.405 Å). These are effective parameters which give good results for the energy and other properties of homogeneous bulk phases. In the present application, they must be regarded as a first approximation. We have addressed this question in greater detail elsewhere [39]. The complete potential function of the interaction for a pair of nitrogen molecules also contains other terms to describe the dispersion, the repulsion and the induction interaction. **We have used the same description of the quadrupole as that used for the nitrogen/zeolite potential model in order to achieve consistency**. The pairwise electrostatic interaction is then a sum of coulombic terms involving two charges pertaining to two different molecules. The long range character of electrostatic interaction is a serious problem for simulation. The minimum image convention [27] requires that the adsorbate-adsorbate interaction cutoff should be less than the half of the smallest dimension of the simulation box which is 20.1 Å if the simulation box is a system of 27 unit cells of orthorhombic silicalite. This cutoff distance is certainly large enough to ensure a good convergence of short range adsorbate-adsorbate interactions but is not sufficient for long range coulombic interactions. There is thus a need to implement the Ewald sum method as described above. Since, we now consider the coulombic interaction between two nitrogen molecules each having a four charge distribution, the self term should be rewritten as [27]:

$$E_3 = \sum_i \left[\left\{ \sum_a^{n_s} \frac{\alpha q_{ia}^2}{\pi^{1/2}} \right\} + \frac{1}{2} \left\{ \sum_a^{n_s} \sum_b^{n_s} q_{ia} q_{ib} \frac{\operatorname{erf}(\alpha d_{ab})}{d_{ab}} \right\} \right] \quad \text{with} \quad a \neq b \tag{14}$$

where n_s is the number of interaction sites on molecule i and d_{ab} is the distance between two interaction sites on the same molecule. Another way to handle long range interaction is to use the reaction field method [27]. This technique requires a knowledge of the dielectric constant of the fluid. This is obviously not known for nitrogen molecules adsorbed in microporous cavities. A way to avoid this problem is simply to consider the dielectric constant as an adjustable parameter. However, we have chosen here to consider the nitrogen molecules in the zeolitic pores as a conductor fluid so that the dielectric constant is taken to be equal to infinity. This approximation has been proven valid in simulation of strongly and moderately polar liquids [41].

Downloaded At: 19:17 14 January 2011

Using the reaction-field technique with this condition, the electrostatic potential can be written (in atomic units):

$$U_{RF} = \frac{1}{2}\sum_i \sum_j q_i q_j \left\{ 1 + \frac{1}{2}\left(\frac{r_{ij}}{r_c}\right)^3 \right\} \tag{15}$$

where r_{ij} is the distance between two interaction sites pertaining to different molecules and r_c the distance cut-off imposed by the minimum image convention. It is clear that such a method, although approximate, is not expensive in terms of CPU time compared to the complete (and exact) Ewald summation technique. In this work, we aim to compare the reaction field method to the Ewald technique for the calculation of nitrogen-nitrogen interactions. The other contributions (short range repulsive inductive and dispersive interactions) are modelled with a two-body form based on two Buckingham potential functions and a polynomial expansion which considers atomic centres. This model of the pair potential for nitrogen has to be considered as an effective potential and was used to reproduce successfully the structure of the adsorbed phase of nitrogen on graphite [26]. The short range potential is:

$$\begin{aligned} U_{sh} &= A_1 \exp(-\alpha_1 r_{ij}) - \frac{B_1}{r_{ij}^6}, \quad r_{ij} > r_1 \\ &= \sum_{n=0}^{4} C_n (r_{ij} - r_0)^n - \frac{B_1}{r_{ij}^6}, \quad r_1 \geqslant r_{ij} \geqslant r_0 \\ &= A_2 \exp(-\alpha_2 r_{ij}) - \frac{B_1}{r_{ij}^6}, \quad r_{ij} < r_0 \end{aligned} \tag{16}$$

where

$$A_1 = 9.261\,205 * 10^7 \text{ K}, \quad \alpha_1 = 4.037 \text{ Å}^{-1}$$

$$A_2 = 1.472\,480 * 10^7 \text{ K}, \quad \alpha_2 = 3.480 \text{ Å}^{-1}$$

$$B_1 = 1.79 * 10^5 \text{ K Å}^6$$

$$C_0 = 415.73\,107 \text{ K}, \quad C_1 = -1446.744\,14 \text{ K Å}^{-1}$$

$$C_2 = 2480.73711 \text{ K Å}^{-2}, \quad C_3 = -2766.5419 \text{ K Å}^{-3}$$

$$C_4 = 1574.2809 \text{ K Å}^{-4},$$

$$r_0 = 3.010\,068 \text{ Å}, \quad r_1 = 3.449457 \text{ Å}$$

Downloaded At: 19:17 14 January 2011

and r_{ij} is the interatomic distance between the atom i pertaining to the first molecule and the atom j pertaining to the second molecule. Freeman [42] has shown that a configuration for which two molecular axes are on the same line, such that the point charges of adjacent nitrogen molecules overlap, yields a considerable negative energy. Furthermore it is known that the Buckingham potential functions passes through a non-physical maximum at very small values of r_{ij} and leading to a negative energy because of the weakness of the exponential function (repulsive energy) at very short distance; this situation is never encountered with the Lennard-Jones function. In order to avoid these unphysical situations, one has to use a hard sphere cutoff: the nitrogen atom centres must not be allowed to come closer than a specified distance chosen at 2 Å.

3. THE GRAND-CANONICAL MONTE-CARLO METHOD

The Grand Canonical Monte-Carlo method is particularly convenient for studying adsorption, because the chemical potential (μ), volume (V), and temperature are fixed in the simulation [7]. The chemical potentials of the adsorbed phase and the gas bulk phase (the Grand Canonical reservoir) are equal at equilibrium. This further enables the pressure to be calculated in the reservoir from an equation of state. Thus the pressure in the reservoir is directly related to the chemical potential of the adsorbed phase. The Grand Canonical formalism for adsorption is close to real experimental conditions in which the Grand Canonical reservoir is simply the gas phase above the zeolite sample in the experimental cell. The ensemble average of the number of molecules in the system, $\langle N \rangle$ (equivalent to the amount adsorbed), is obtained directly from the simulation. By running the simulation at various bulk pressures (*i.e.* at various values of μ), one can obtain the adsorption isotherm which can be directly compare to the experimental curve. From a technical point of view, three different Monte-Carlo trials are attempted in this type of simulation: translational and/or rotational displacements of a (randomly chosen) molecule within the system (canonical trials in the original Metropolis algorithm [43]), creations of a new molecule (at random position and orientation) and attempts to delete an existing molecule. The acceptance criteria for all these Monte-carlo trials are such that molecular configurations are generated within the Grand Canonical formalism with probabilities proportional to their Boltzmann weighting factor. In addition, it is possible to calculate the isosteric heat of adsorption (q_{st}) and its two adsorbate-adsorbate and adsorbate-zeolite contributions at each pressure

Downloaded At: 19:17 14 January 2011

value and compare the plot q_{st} versus $\langle N \rangle$ directly with the microcalorimetric curve. Finally, one gets structural information on the adsorbed phase by calculating singlet and pair distribution functions. It should be mentioned that experimental data yields an excess number of molecules adsorbed, not $\langle N \rangle$. At low temperatures and in small pores, the correction from absolute to excess adsorption is however negligible.

4. RESULTS AND DISCUSSION

4.1. Adsorption of Argon at 77 K

The results presented in this work are complementary to those reported earlier in reference [35] which dealt with GCMC simulations of adsorption of rare gases in silicalite at various temperatures. In this previous work, the simulated adsorption isotherms were calculated over moderate pressure domains using the same adsorbate/zeolite potential model as that presented above and assuming a rigid zeolite framework. In the particular case of argon, the adsorption isotherm at 77 K was simulated between $5 \cdot 10^{-3}$ Pa and 100 Pa only. However, this pressure range extends well beyond the critical pressure at which the experimentally observed step occurs (7 Pa) [10, 11]. The simulated isotherm did show no step in the pressure range considered and the authors attributed the step to a adsorbate-induced structural transition (or distortion) of the zeolite framework (accompanied with some rearrangements of the adsorbed phase itself) since the zeolitic structure was kept rigid during simulation runs. This interpretation is in contradiction with the original experimentalist view *i.e.* a fluid to crystalline solid transition for the adsorbed phase only [17]. In this paper, we present new GCMC results for the adsorption of argon in silicalite at very high pressure *i.e.* up to 10^7 Pa. Surprisingly, a step in the adsorption isotherm at 77 K is obtained in the simulated curve between 25 to 31 argon atoms per unit cell of zeolite in agreement with the experiment [10, 11, 15, 16, 17]. However, a straightforward analysis of the simulated curve reveals important differences with the experimental isotherm (see Fig. 2): (i) the slope of the simulated curve at the transition is smaller than the slope of the experimental isotherm step which is nearly vertical; (ii) the transition pressure is $P_{tr} = 5 \cdot 10^5$ Pa which is several orders of magnitude higher than that observed experimentally (iii) upon desorption, the simulated isotherm is perfectly reversible and exhibits no hysteresis loop in contrast with experiment. The two first observations suggest that the mechanism(s) responsible

Downloaded At: 19:17 14 January 2011

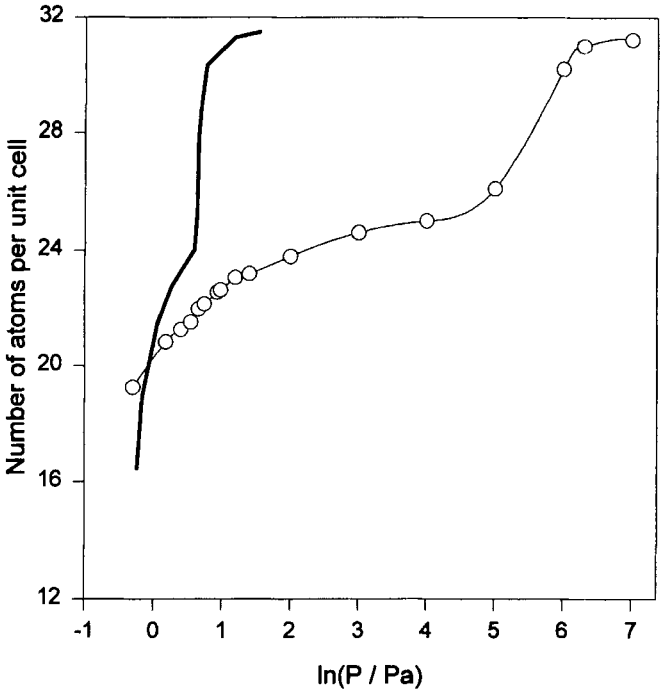

FIGURE 2 Adsorption isotherm for argon in silicalite at 77 K, (solid line) experiment [44], (open circle) GCMC simulation (this work).

for the experimentally observed transition may not be properly described in the adsorption model used in the simulation. This is supported by the analysis of the isosteric heat curve, *i.e.* the curve giving the evolution of q_{st} as a function of coverage presented in Figure 3 which compares both simulated and experimental curves. The two contributions to the total simulated heat curve, namely the adsorbate/zeolite and the adsorbate/adsorbate components, are also shown. As discussed in reference [35], the experimental transition step from 24 to 31 Ar/uc corresponds to the end of a plateau and a final two-stage decrease of the experimental isosteric heat curve; the increase of q_{st} occurs *prior* to the transition step (*i.e.* from 18 to 22 Ar/uc). The simulated heat curve does not exhibit such an evolution: it smoothly increases up to 23 Ar/uc and decreases monotically until the maximum loading (31 Ar/uc) is reached. It has been demonstrated recently that higher order three-body potential terms involving three Ar atoms and two Ar and a zeolite species, lower the adsorbate-adsorbate contribution to the total isosteric heat [39], yielding good agreement between simulation

Downloaded At: 19:17 14 January 2011

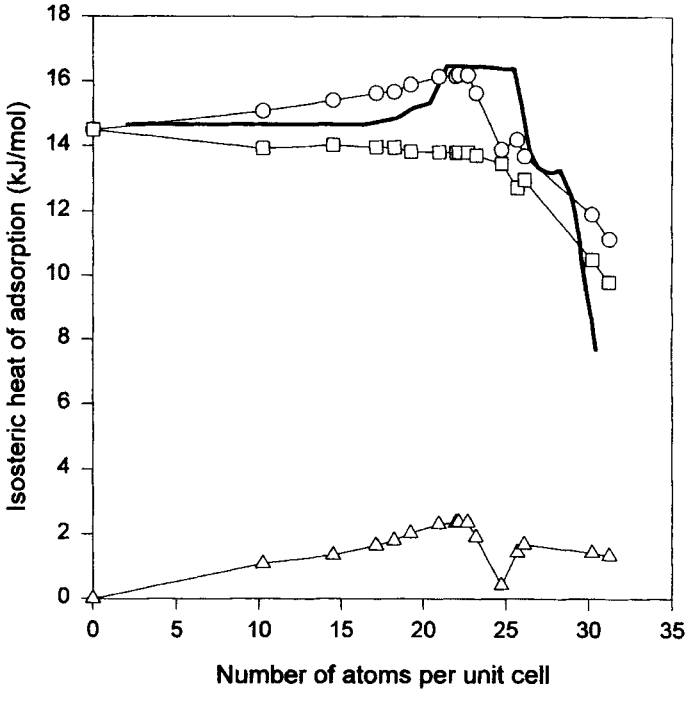

FIGURE 3 Isosteric heat curve for argon in silicallite at 77 K: (solid line) experimental data [44], (circle) total simulated isosteric heat, (square), adsorbate-zeolite contribution, (triangle) adsorbate-adsorbate contribution.

and experiment from 0 to 23 Ar/uc. In this range of loading, the (simulated) adsorbate/zeolite contribution constantly decreases while the adsorbate-adsorbate component constantly increases. The latter reaches a maximum at 23 Ar/uc and starts decreasing up to 25 Ar/uc (see Fig. 3). The simulated isotherm step corresponds to the final (strong) decrease of the adsorbate-zeolite heat component which is caused by repulsive interactions between the zeolite walls and the adsorbates when approaching the maximum loading; the adsorbed phase being stabilized by the external chemical potential [35]. Between 25 to 31 Ar/uc (*i.e.* the isotherm step), the adsorbate-adsorbate heat contribution starts to increase again showing that the transition observed in the simulation is driven by adsorbate-adsorbate interactions. Finally, the adsorbate-adsorbate heat contribution decreases at maximum loading showing repulsive interactions between adsorbates themselves.

Recently, Llewellyn *et al.* [17] have measured neutron diffraction spectra at various argon loading in silicalite at 77 K: the appearance of new structures in the diffraction spectra after the transition was attributed to an

Downloaded At: 19:17 14 January 2011

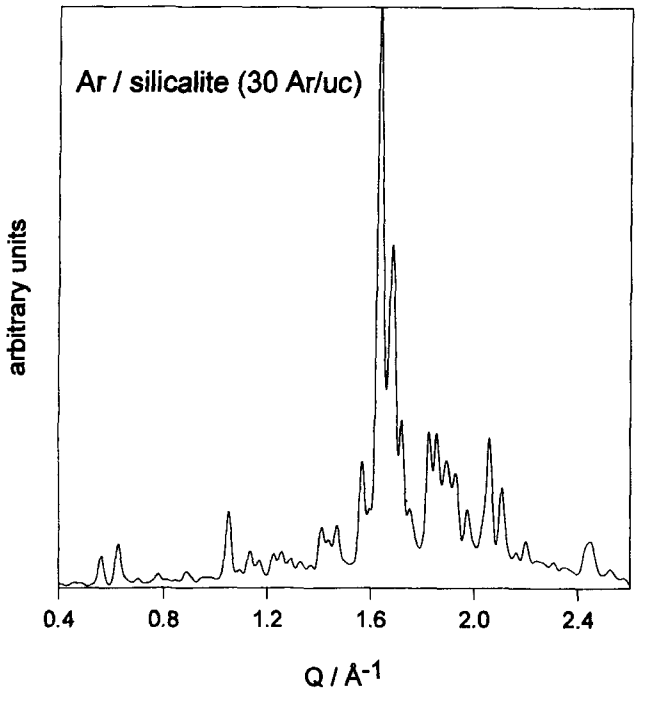

FIGURE 4 Simulated ^{36}Ar diffraction spectrum at 30 Ar/uc.

Downloaded At: 19:17 14 January 2011

ordering of the argon atoms from a fluid disordered phase to a crystalline solid phase. We have calculated diffraction spectra for various loadings using the equilibrium adsorbate configuration output from the GCMC code. The effect of the system size and the role of the different parts of the microporous network of silicalite were described to some length in reference [35]: here we have considered an argon configuration generated from a 27 silicalite unit cell system (*i.e.* ≈ 830 argon atoms). Empty zeolite and 24 Ar/uc spectra can be found in reference [35]. We present in Figure 4, the diffraction spectrum at high loading (≈ 30 Ar/uc) after the isotherm step. Most of the peaks present in the experimental spectrum are present in the simulation diffractogram although there are some differences: (i) some peaks characteristic of the sorbed phase are not as intense on the simulated spectrum as they are on the experimentally, especially at $Q = \{1.8, 1.95\ \text{Å}^{-1}\}$ (ii) some peaks at $Q = \{1.6, 1.8\ \text{Å}^{-1}\}$ attributed to the zeolite structure which experimentally show a splitting remaining singlet in the simulation. The conclusions from diffraction are consistent with those given in reference [35] namely: (i) the high loading adsorbed phase taken from the simulation is not as ordered as it is in experiment, (ii) the zeolite structure shows some

structural modifications experimentally which are not taken into account in the simulation since the framework is kept rigid. Recently, Coulomb and Tosi-Pellenq [18,44] have measured neutron diffraction spectra for ^{40}Ar adsorbed in silicalite at various loadings. Since the ^{40}Ar isotope has a very small coherent length, one can follow the evolution of the zeolitic lattice during adsorption. The ^{40}Ar diffraction spectrum recorded at 77 K after the isotherm step is different than that obtained at 24 Ar/uc (*i.e.* before the transition step). It is interesting to note that the differences between the two spectra occur in the peaks at $Q = (1.6, 1.8\ \text{Å}^{-1})$ *i.e.* the same peaks as those modified during the adsorption of ^{36}Ar. On the other hand, the intense and narrow peaks that occur with ^{36}Ar at high loading at $Q = (1.8, 1.95\ \text{Å}^{-1})$ are not seen on the high loading ^{40}Ar diffraction spectrum. This strongly supports the view that all changes between the 24 Ar/uc and 30 Ar/uc spectra can be attributed to changes in the zeolite structure. It is also interesting to note that the same set of peaks characteristic of the zeolitic framework (for $Q = 1.6, 1.85\ \text{Å}^{-1}$ or $2\theta = 23–25°$), are affected by the adsorption (at room temperature) of aromatic molecules such as para-xylene in silicalite [46]. In the case of para xylene adsorption in silicalite, Van Koningsveld *et al.* [8] have demonstrated that the changes in the zeolitic framework were the consequence of a crystalline phase transition. The striking analogy between argon adsorption at 77 K and para xylene adsorption at 195 K, as far as the isotherm and heat curve are concerned, was reported to some length in reference [35]. Furthermore, it is worth mentioning that for adsorbate molecules which do not give stepped isotherms such as methane at 77 K [17] or cyclohexane at 300 K [48], the zeolite framework structure is fully preserved upon adsorption. The extent by which the silicalite crystal is affected by the adsorption of argon at 77 K awaits further work. The analysis of the singlet distribution functions gives some more indications on the mechanism of the transition observed in the simulation. It can be seen from Figure 5 that the density distribution for the 24 Ar/uc phase in the straight channels is different from that for the 31 Ar/uc phase which shows new peaks. Conversely, the density in the zig-zag channels remains essentially the same for both the 24 and the 31 Ar/uc phases. This indicates that the transition only affects the argon atoms adsorbed in the straight channels. In fact, the comparison with potential maps for one argon interacting with the zeolite structure [29] leads to the conclusion that the argons first adsorb in the adsorption sites to form a phase commensurate with the site distribution (24 adsorption sites per unit cell) and those in the straight channels are then pulled off these sites. This frees void space which can then be filled by six to

Downloaded At: 19:17 14 January 2011

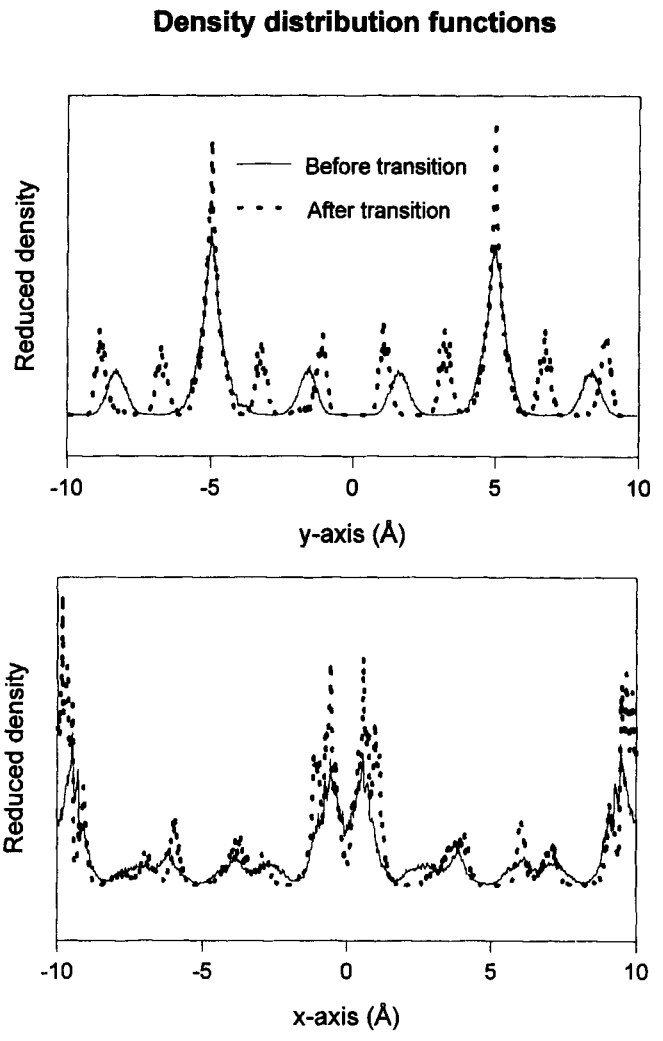

FIGURE 5 Density distribution functions along x-axis (sinusoidal channels) and along the y-axis (straight channels), (solid line) before transition, (dotted line) after transition.

seven more molecules. From an energetic point of view, the transition between the two states results from a subtle balance between the adsorbate-zeolite and the adsorbate-adsorbate interactions: the adsorbate-zeolite potential hypersurface, as described by the PN potential function used in this work, [29, 30, 37, 38] is smooth enough for the adsorbate/adsorbate interaction to be able to pull the adsorbates in the straight channels off their sites at the transition chemical potential. It should also be mentioned that an

Downloaded At: 19:17 14 January 2011

adsorbate/zeolite potential function which gives a more corrugated energy hypersurface (as is the case for a Lennard-Jones function parametrized following Kiselev's method [35]) yields a continuous adsorption *i.e.* a Langmuir-type adsorption isotherm [35, 37]. Finally, the Ar-Ar pair correlation functions given in Figure 6 show that the Ar-Ar nearest neighbour distance is the same for both the 24 and 31 Ar/uc phases. It is interesting to note that this Ar-Ar distance (3.55 Å) is shorter than that observed for the argon crystalline fcc phase (3.76 Å) but larger than the argon hard-sphere diameter ($\sigma = 3.40$ Å). This is consistent with the behaviour of the adsorbate-adsorbate contribution to the total isosteric heat of adsorption (see Fig. 3). The high loading pair correlation function also shows some new peaks (second and third nearest neighbours) which are more clearly defined than in the pair correlation function at 24 Ar/uc. Thus, the high loading phase is more structured than the 24 Ar/uc phase, although both phases show the same nearest neighbour distance. This feature, along with the in-site/off-site transition mechanism, indicates that the high-loading argon phase in silicalite is

Downloaded At: 19:17 14 January 2011

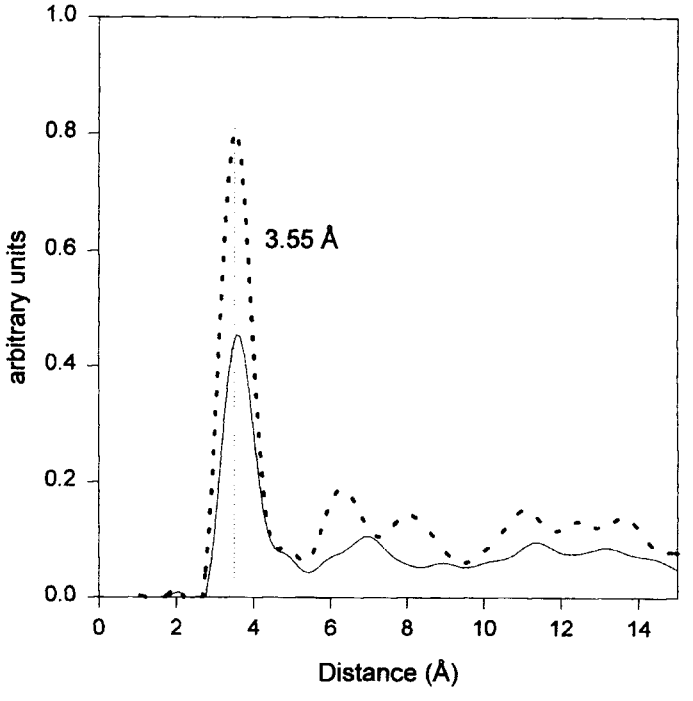

FIGURE 6 Ar-Ar Pair correlation function, (solid line) before transition, (dotted line) after transition. The vertical line corresponds to $R_{eq} = 3.55$ Å: $\sigma_{Ar\text{-}Ar} = 3.405$ Å $< R_{eq} < 3.76$ Å (fcc solid argon phase).

not a one dimensional phase. Recently, Boutin *et al.* [37] have been able to reproduce, using GCMC simulation, the experimentally observed step [44, 56] in the adsorption isotherm of methane in $AlPO_4$-5 (a porous aluminophosphate). This step in the $CH_4/AlPO_4$-5 isotherm results from an on-site/off-site transition of the adsorbed phase, similar to that found for argon in this work. Finally, it is interesting to mention the Molecular Dynamics study of Demontis *et al.* [54] on the influence of methane adsorption on a flexible silicalite structure at room temperature: this work shows that a loading of 24 CH_4 molecules per unit cell induces change in the zeolitic framework consistent with the structural monoclinic-orthorhombic transition above mentioned although there is no experimental evidence of the step/hysteresis phenomenon (neither at 77 K [17] nor at room temperature) allowing the docking of 24 CH_4 molecules per silicalite unit cell [52, 17, 55].

4.2. The Adsorption of Nitrogen

Figure 7 presents the simulated adsorption isotherm at 77 K. The experimental isotherm obtained by Tosi-Pellenq [44] at 77 K shows several features: a first step, which is observed at low pressure from 20.5 to 21.8 nitrogen molecules per unit cell. This step was attributed to a 'fluid to lattice-fluid-like transition' by Llewellyn *et al.* [19] although Llewellyn *et al.* found this first step between 23 and 25 nitrogen molecules per unit cell. The experimental isotherm shown in Figure 7 also exhibits a second step which occurs at higher pressure from 22 to 28 nitrogen molecules per unit cell. The simulated isotherm reproduces only the first step with a correct amplitude but not at the correct pressure: the experimental pressure for the first step occurs at about 200 Pa, the transition pressure obtained in the simulation is 2000 Pa. Coulomb [52] has observed this step at 250 Pa at 62 K; so that the step will be shifted to higher pressure at 77 K in better agreement with the simulation. The maximum amount adsorbed in the simulated isotherm is 22 nitrogen molecules per unit cell. The simulation does not reproduce the second experimental step whose magnitude (7 molecules) is much larger than that of the first low pressure step (2 molecules). Note that the simulated isotherm is reversible and exhibits no hysteresis loop. The simulated isosteric heat curve and its experimental counterpart are presented in Figure 8. It is clear that the two curves are in good agreement and are similar in shape up to 22 molecules per unit cell; in particular, both show a sudden variation of the isosteric heat of adsorption between 20 and 22 N_2/uc *i.e.* during the first isotherm step. The two contributions to the

Downloaded At: 19:17 14 January 2011

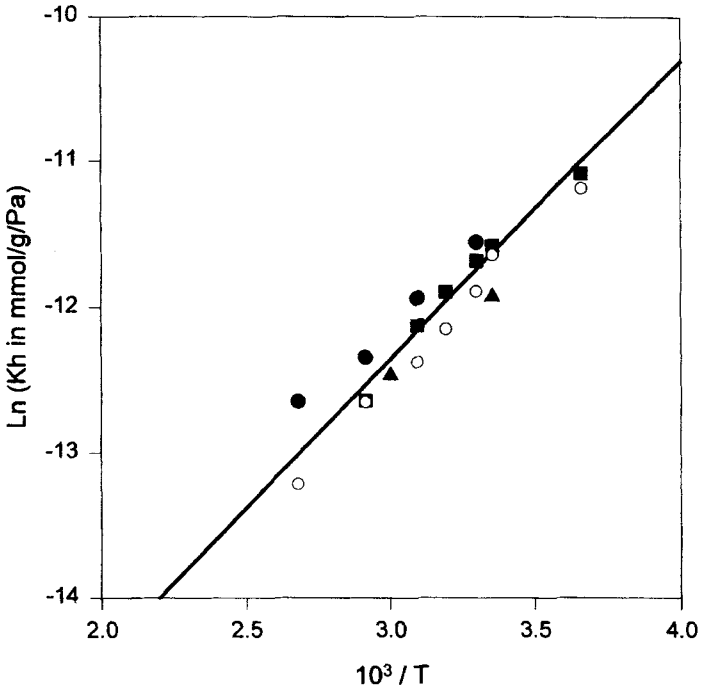

FIGURE 7 Adsorption isotherm for nitrogen in silicalite at 77 K, (solid line) experiment [44], (open circle) GCMC simulation (this work), insert: low pressure adsorption isotherm.

Downloaded At: 19:17 14 January 2011

total isosteric heat of adsorption are also presented in Figure 8. The adsorbate-adsorbate contribution increases up to 20 N_2/uc and decreases during the isotherm step which means that the molecular mechanism responsible for the first isotherm step is not favourable to adsorbate-adsorbate interactions. Conversely, the adsorbate-zeolite contribution shows a sudden variation during the isotherm transition. Thus from an energetic point of view, one may conclude that the first isotherm step is driven by the adsorbate-zeolite interactions. The experimental heat curve also exhibits an exothermic signal from 24 to 31 molecules per unit cell which is not reproduced theoretically since the maximum amount predicted in the simulation is 22 nitrogen molecules per unit cell. It is interesting to note that the microcalorimetric signal for the second isotherm step is very similar in shape to that found for argon: in each case, the isotherm step corresponds to a plateau and a final decrease of the heat curve. Pair correlation functions are given in Figure 9 for the molecular configurations at 20 and 22 N_2/uc

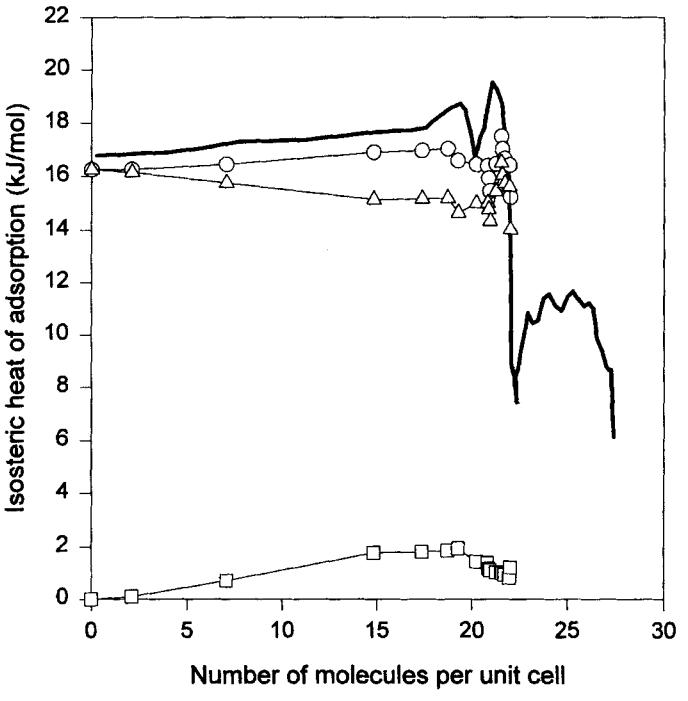

FIGURE 8 Isosteric heat curve for nitrogen in silicalite at 77 K: (solid line) experimental data [44], (circle) total simulated isosteric heat curve, (triangle) adsorbate-zeolite contribution, (square) adsorbate-adsorbate contribution.

respectively. Before the transition, the probable distance between neighbouring molecules is 4 Å which corresponds to the intermolecular distance encountered in solid nitrogen. After the transition, the nitrogen-nitrogen distance has decreased to 3.8 Å. This means that the adsorbed phase is very dense and that the molecules are in close (repulsive) contact. The decreasing $N_2 - N_2$ component of the total isosteric heat curve (Fig. 8) between 20 to 22 N_2/uc supports this result. Furthermore, one can see from Figure 9 that the 22 N_2/uc pair correlation function shows well defined peaks at 7 and 10 Å. These peaks indicate that the 22 N_2/uc phase is more structured than that at 20 N_2/uc, which only shows a second-nearest-neighbour peak at 7.8 Å. These new structures, at intermediate distances, may be expected for an ordered solid-like phase. However, the void volume available in the zeolite channels does not allow the formation of a 3D nitrogen solid phase even at the channel intersections. In fact the 22 N_2 pair correlation function simply shows that there is a densification of the adsorbed phase since the first and

Downloaded At: 19:17 14 January 2011

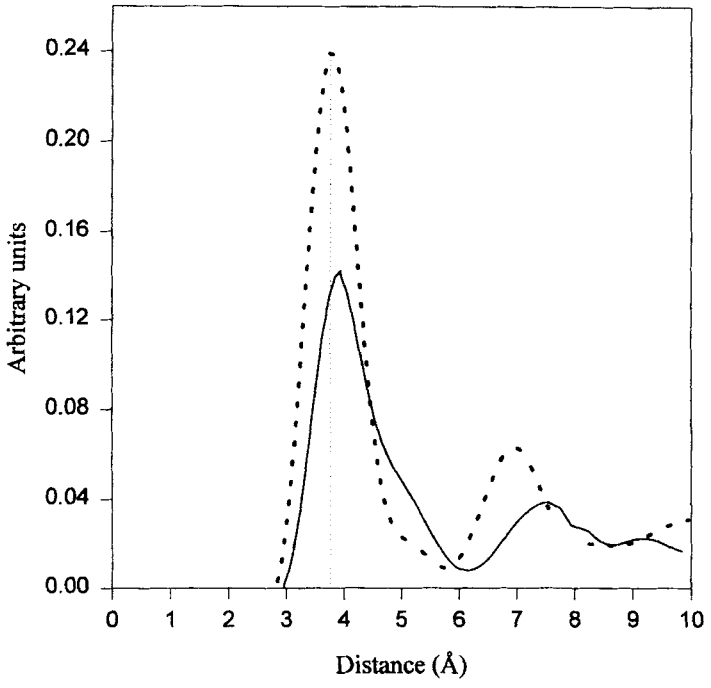

FIGURE 9 Ar-Ar Pair correlation function, (solid line) before transition, (dotted line) after transition. The vertical line corresponds to $R_{eq} = 3.80$ Å.

second nearest-neighbour peaks are shifted from 4 to 3.8 Å and from 7.8 to 7 Å respectively. It is interesting to note that such a densification also occurs for argon adsorbed in silicalite *prior* to the transition step (see Fig. 6). The analysis of snapshot pictures (Fig. 10) and angle correlation functions show that the molecules tend to be parallel within the channels with one atom pinned onto the zeolitic wall: the angle correlation function at 20 molecules per unit cell shows a broader distribution than that obtained at 22 N_2/uc. Figure 11 presents the singlet distribution functions for the two types of channels before and after the transition. It is clear that the isotherm step corresponds to changes in the distribution of molecules adsorbed in the sinusoidal channels only. The corresponding 22 N_2 density plot shows narrow peaks compared to those found for the 20 N_2 molecule phase, indicating a very localized phase, in which the molecules are at the adsorption sites. The molecules adsorbed in the straight channels remain in site during the transition. At 22 N_2/uc, all molecules are in adsorption sites and the adsorbed phase is commensurate with the site distribution in a similar manner to that found for 24 Ar phase (see above). One may conclude that the

Downloaded At: 19:17 14 January 2011

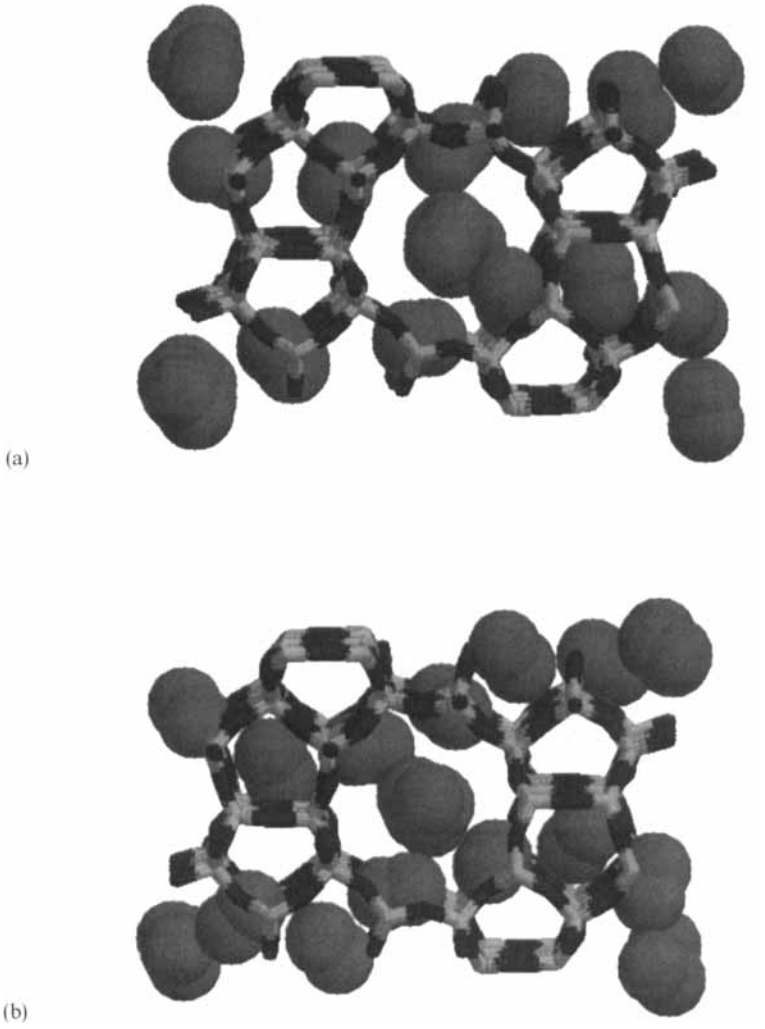

FIGURE 10 Snapshots configurations (a) at 20 nitrogen molecules per unit cell in the (x, z) plane, at 22 nitrogen molecules per unit cell in the (x, z) plane.

first step in the 77 K nitrogen isotherm corresponds to a transition from a disordered fluid to a localized commensurate phase for the molecules in the sinusoidal channels accompanied by the adsorption of two more molecules per unit cell. Thus the origin of the first step in the nitrogen isotherm at 77 K is different from that found for argon (on-site/off-site transition for adsorbates in the straight channels most probably accompanied by distortions of the zeolitic framework). As far as the second transition from 24 to 31 N_2/uc

Downloaded At: 19:17 14 January 2011

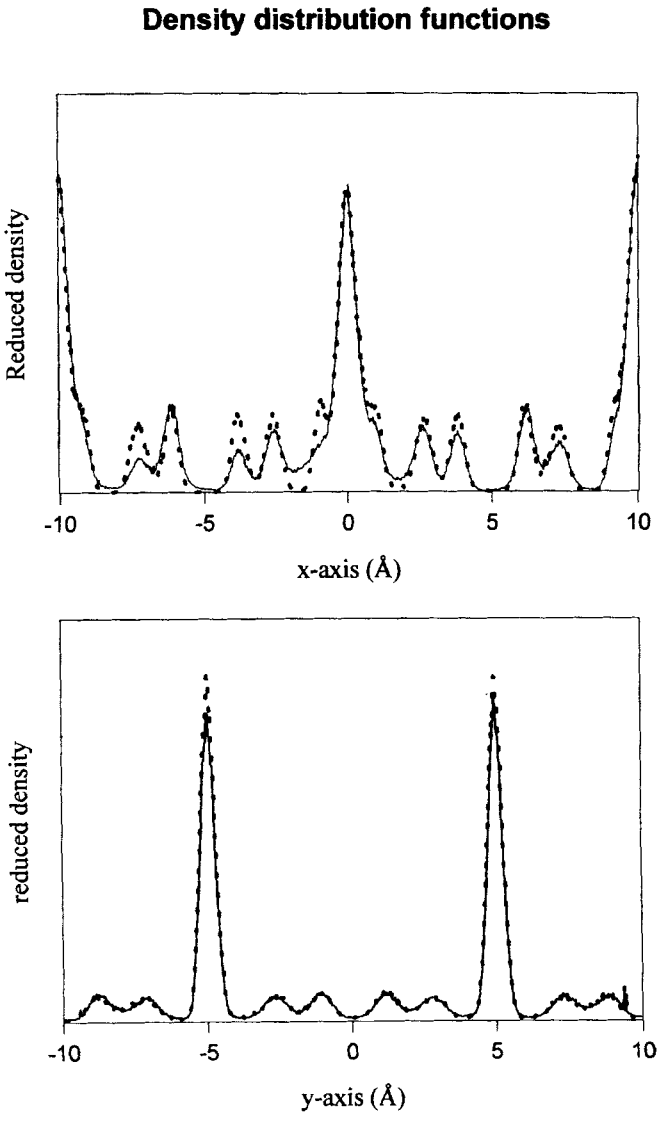

FIGURE 11 Density distribution functions along *x*-axis (sinusoidal channels) and along the *y*-axis (straight channels), (solid line) before transition, (dotted line) after transition.

is concerned, we have already noted the similarity between the isosteric heat curve for nitrogen and for argon over the same loading range. Recent neutron diffraction experiments of Llewellyn *et al.* [19] have shown that the phase at 31 N_2/uc is characterized by narrow and intense peaks indicative

Downloaded At: 19:17 14 January 2011

of a long range order. The high-loading diffraction spectrum also exhibits the same modifications of the peaks characteristic of the zeolitic structure as that found for argon; it was concluded by the experimentalists that nitrogen adsorption at 77 K induces changes of the zeolitic framework from its initial monoclinic symmetry to an orthorhombic framework [10]. This further supports the hypothesis of distortions of the zeolitic structure occurring upon argon adsorption. Finally, it is interesting to note that both the reaction field (in the conducting fluid approximation) and the Ewald techniques used in the calculation of the long range coulombic part of the nitrogen-nitrogen intermolecular potential, give similar results for the adsorption isotherm and the isosteric heat curve.

5. CONCLUSION

We have derived in this work a full scale potential function for adsorption of nitrogen in silicalite, based on the methodology reported earlier for rare gases and non polar molecules in various zeolites [29, 35, 37, 38]. The new potential function for the nitrogen/silicalite system accurately predicts the isosteric heat of adsorption at zero-coverage and Henry's law constants at all temperatures.

We have compared GCMC simulation results for argon and for nitrogen adsorbed in silicalite against several experimental data (adsorption isotherm, isosteric heat of adsorption, and neutron diffraction spectra). The argon isotherm step was originally interpreted as the signature of a phase transition from a fluid to a solid phase [17]. This conclusion seems at the first sight to be in agreement with neutron diffraction spectra on which new and intense bands are described as characteristic of a solid-like organisation of the adsorbed phase. It was important, in reconsidering experimental data, to realize that the isotherm step corresponds to an evolution at constant isosteric heat followed by a final decrease of the q_{st}. The newly introduced adsorption potential model (PN) performs well at low coverage in predicting thermodynamic data and does reproduce the observed step. Although, the magnitude of the simulated isotherm step is in good agreement with experiment, the transition pressure found in the simulation is several orders of magnitude higher than that obtained experimentally. The step in the simulated isotherm corresponds to an on-site/off-site transition for adsorbates in the straight channels. We have also compared simulated neutron diffraction spectra with experiment for the argon/silicalite system, using the equilibrium configurations obtained at maximum loading. The results are

Downloaded At: 19:17 14 January 2011

encouraging since new bands occur at the correct positions on the simulated spectra. Another interesting feature which arises when comparing simulated neutron diffraction with experiment is the evolution of the zeolite structure upon adsorption. This was confirmed with the ^{40}Ar experiment of Coulomb and Tosi-Pellenq [18,44]: the zeolite structure shows some lattice distortions occurring simultaneously with the isotherm step. Since no structure refinement has been made under adsorption of the molecules studied here, it is not possible to evaluate the extent of the structural modifications of the zeolite needed to explain the gap in pressure between simulation and experiment. The comparison between the calculated and the experimental isosteric heat curve also supports this hypothesis. Finally the analysis of the pair correlation functions at 24 and 31 Ar/uc shows that both phases are very dense in terms of average nearest neighbour distance, which is found to be less than that encountered in solid fcc argon. In the case of nitrogen, the simulated isotherm reproduces well the observed first step on the experimental isotherm. This step occurs simultaneously with large variations of the isosteric heat of adsorption. The simulated isosteric heat curve is in good agreement with experiment. We have shown that the first isotherm step corresponds to a phase transition from a disordered fluid to a localized commensurate phase for the molecules adsorbed in the sinusoidal channels. This also corresponds to a densification of the adsorbed phase. The nitrogen/silicalite potential model used in the simulation, does not predict the second step on the nitrogen isotherm whose magnitude is comparable to that encountered with argon. Diffraction experiments seem to support the view that zeolite distortions occur during the adsorption of nitrogen at 77 K [52, 10].

The possibility of zeolite relaxation has been recently considered by Mersmann *et al.* [47] to explain isotherm steps and hysteresis: they developed phenomenological models based on the concept of a 'lattice mediated interaction'. We therefore propose that the observed isotherm step for argon is a consequence of an adsorbent framework transition which minimises the free energy of the total system once it has reached the substep loading. A mechanism can be proposed along the following lines: for some adsorbate species there will be a misfit between adsorbate molecules and pore walls, such that a small expansion of the adsorbent pore would enable further molecules to squeeze into the pore space, the increase in lattice energy being compensated by a reduction in adsorbate energy. Following this idea, the zeolite structure could even contract to reduce the misfit with adsorbed molecules; in this case there will be no step on the isotherm, which will remain of type I with the corresponding heat curve (case of xenon, methane

Downloaded At: 19:17 14 January 2011

and cyclohexane). This mechanism implies an energy compensation which may explain why the beginning of the isotherm step occurs at nearly constant isosteric heat. The zeolite relaxation is most certainly accompanied by a rearrangement of the adsorbed molecules. This would be consistent with neutron diffraction spectra at maximum loading which indicate a long-range ordering of the adsorbate phase (intense and narrow peaks) which occurs simultaneously with the modification of peaks characteristic of the crystal structure. All these features would be also true for the second step in the nitrogen isotherm. Both the argon and nitrogen simulated isotherms are reversible and do not shown any hysteresis phenomenon. This is in contradiction with experiment for nitrogen, but in agreement with experiment for argon. Since the hysteresis loop is absent from the argon simulated isotherm, it is reasonable to envisage the hysteresis phenomenon as a further consequence of the zeolite relaxation. This is supported by the recent solid state NMR experiments of Janchen *et al.* [49] for methanol adsorbed in $AlPO_4$-18 (a microporous aluminophosphate) who preformed ^{27}Al NMR experiments coupled with methanol adsorption isotherm and heat curve measurements at room temperature. The adsorption isotherm of methanol exhibits the step/hysteresis phenomenon. They have shown that the zeolitic structure $AlPO_4$-18 exhibits a lattice distortion upon adsorption which remains during desorption until the hysteresis loop closes; the original crystal structure being finally fully recovered.

The idea of zeolite relaxation or distortion is consistent with the classification of zeolitic structures proposed by Baur [51]: zeolitic frameworks are described as collapsible or as noncollapsible. Collapsible frameworks are those in which, upon a change in volume, all hinges (between two rigid SiO_4 tetrahedra) corotate while the framework distorts. Noncollapsible framework are those where hinges antirotate when the unit cell volume is changed. Both types are flexible although the amount of angular variations at the hinges is larger for the noncollapsible than for the collapsible frameworks which show the largest changes in their unit cell volume. Individual oxygen atoms can be displaced by up to 0.5 Å. According to this classification, silicalite is an anticollapsible framework since the analysis of the ^{40}Ar spectra show very little volume change (for the unit cell) when going from the 24 to the 31 Ar/uc phase [18,44]. To proceed further, the atomic mechanism of the zeolite relaxation can be approached through the soft mode theory for solid-solid phase transitions. Van Koningsveld *et al.* [8] have shown that the temperature induced monoclinic-orthorhombic transition of ZSM5 zeolites (empty) is ferroelastic *i.e.* at the critical temperature

Downloaded At: 19:17 14 January 2011

(room temperature), the stress required to transform the lattice from one to another ferroelastic domain vanishes. Below the critical temperature, an activation energy is required. At the ferroelastic transition, one of the (acoustic) lattice vibration modes becomes soft *i.e.* its corresponding frequency becomes zero. This soft mode allows displacement of framework atoms. The transition would be second order. If however more than one mode is involved, the transition would be first order and it would not be necessary for any frequencies to approach close to zero but simply for them to be several orders of magnitude lower compared to the other modes not involved [53]. Under adsorption at a temperature below the critical temperature of the monoclinic-orthorhombic transition, the coupling between zeolite atoms and adsorbate molecules (at a sufficiently high loading corresponding to the intermediate plateau on the adsorption isotherm) would be strong enough to approach an instability of the crystal which would give rise to a relaxation of the zeolite framework; the activation energy being provided by the adsorbate-zeolite interactions.

Downloaded At: 19:17 14 January 2011

Acknowledgements

The authors would like to thank Nathalie Tosi-Pellenq, Jean-Paul Coulomb and Yves Grillet for communicating their results from ^{40}Ar neutrons spectra prior to publications and for fruitful discussions.

References

[1] Gregg, S. J. and Sing, K. S. W. (1967) in "*Adsorption and Porosity*", Academic Press.
[2] Evans, R. and Tarazona, P. (1984) "Theory of condensation in narrow capillaries", *Phys. Lett. Rev.*, **52**, 847.
[3] Kierlick, E., Rosinberg, M. L. (1990) "Free-energy density functional for the inhomogeneous hard sphere fluid, application to interfacial adsorption", *Phys. Rev. A*, **42**, 3382.
[4] Ruthowsky, J., Zukal, A., Franke, O. and Shulz-Ekloff, G. (1994) "Adsorption on MCM-41 mesoporous molecular sieves", *J. Chem Soc. Faraday Trans.*, **90**, 2821.
[5] Balbuena, P. B. and Gubbins, K. E. (1994) "The effect of the pore geometry on adsorption behaviour", in "*Characterization of Porous Solids III*", J. Rouquerol, F. Rodriguez-Reinoso, Sing, K. S. W. and Unger, K. K. eds., Studies in Surface Science and Catalysis, Elsevier, **87**, 41.
[6] Mitchell, M. C., Mc Cormick, A. V. and Davis, H. T. (1995) "Prediction of adsorption of xenon in zeolite NaA with molecular density functional theory", *Z. Phys. B*, **97**, 353.
[7] Nicholson, D. and Parsonage, N. G. (1982) in "*Computer Simulation and the Statistical Mechanics of Adsorption*", Academic Press, New York.
[8] van Koningsveld, H., Trunistra, F., van Bekkum, H. and Jansen, J. C. (1989) "The location of p-xylene in a single crystal of zeolite H-ZSM-5 with a new sorbate-induced orthorhombic framework symmetry", *Acta Crystal.*, **B45**, 423.

[9] Maglara, E., Pullen, A., Sullivan, D. and Conner, W. C. (1994) "Characterization of microporous solids by adsorption: measurement of high resolution adsorption isotherms", *Langmuir*, **10**, 4167.
[10] Reichert, H., Muller, U., Unger, K. K., Grillet, Y., Rouquerol, F., Rouquerol, J. and Coulomb, J. P. (1991) "Sorption of argon and nitrogen on network types of zeolites and aluminophosphates", *Characterization of Porous Solids II*, F. Reinoso *et al.*, eds., Studies in Surface Science and Catalysis, Elsevier, **62**, 535.
[11] Muller, U., Reichert, H., Robens, E., Unger, K. K., Grillet, Y., Rouquerol, F., Rouquerol, J., Dongfeng Pan, A. and Mersmann, A. (1989) "High resolution sorption studies of argon and nitrogen on large crystal of microporous zeolite ZMS-5", *Fresenius Z. Anal. Chem.*, **333**, 433.
[12] Sing, K. S. W. and Unger, K. K. (1993) "Nitrogen adsorption by silicalite and ZSM-5", *Chem. and Ind.*, 165.
[13] Hathaway, P. E. and Davis, M. E. (1990) "High resolution quasi-equilibrium sorption studies of molecular sieves", *Catalysis Letters*, **5**, 333.
[14] Webb, S. W. and Conner, W. C. (1991) "Sorption of gases on microporous solids: pore size characterization by gas adsorption", in *Characterization of Porous Solids II*, Reinoso, F. *et al.*, eds., Studies in Surface Science and Catalysis, Elsevier, **62**, 535.
[15] Borghard, W. S., Reichman, P. T. and Sheppard, E. W. (1993) "Argon sorption in ZSM-5", *J. of Catalysis*, **139**, 19.
[16] Saito, A. and Foley, H. C. (1995) "High resolution nitrogen and argon adsorption on ZSM-5 zeolites: effects of cation exchange and Si/Al ratio", *Microp. Mat.*, **3**, 543.
[17] Llewellyn, P. L., Coulomb, J. P., Grillet, Y., Patarin, J., Lauter, H., Reichert, H. and Rouquerol, J. (1993) "Adsorption by MFI-type zeolites examined by isothermal microcalorimetry and neutron diffraction, part 1; argon, krypton and methane", *Langmuir*, **19**, 1846.
[18] Coulomb, J. P. and Tosi-Pellenq, N. (1993) private communication.
[19] Llewellyn, P. L., Coulomb, J. P., Grillet, Y., Patarin, J., Andre, G. and Rouquerol, J., "Adsorption by MFI-type zeolites examine by isothermal microcalorimetry and neutron diffraction, part 2: nitrogen and carbon monoxide", *Langmuir*, **19**, 1852.
[20] Conner, W. C., Ferrero, M., Bonardet, J. and Fraissard, J. (1993) "First low-temperature ^{15}N NMR study of nitrogen physisorption and condensation in microporous solids", *J. Chem. Soc. Faraday Trans.*, **89**, 833.
[21] Bonardet, J., Fraissard, J., Unger, K. K., Kumar, D., Ferrero, F., Ragle, J. and Conner, W. C. (1994) "The use of ^{15}N NMR for the understanding of nitrogen physisorption", Rouquerol, J., Reinoso-Reinoso, F., Sing, K. S. W. and Unger eds, K. K. (1994) Studies in Surface Science and Catalysis, Elsevier, **87**, 41.
[22] Buckingham, A. D. (1967) "Permanent and induced molecular moments and long range intermolecular forces" *Adv. Chem. Phys.*, **12**, 107.
[23] White, J. C. and Hess, A. C. (1993) "Periodic Hartree-Fock study of siliceous mordenite", *J. Phys. Chem.*, **97**, 6398.
[24] Price, S. L. (1986) "The limitation of isotropic site-site potential to describe $N_2—N_2$ intermolecular surface", *Mol. Phys.*, **58**, 651.
[25] Berns, R. M. and van der Avoird, A. (1980) "$N_2—N_2$ interaction potential from *ab initio* calculation with application to the structure of $(N_2)_2$", *J. Chem. Phys.*, **72**, 6107.
[26] Kuchta, B. and Etters, R. D. (1987) "Calculated properties of monolayer and multilayers N_2 on graphite", *Phys. Rev. B*, **36**, 3400.
[27] Tildesley, D. and Allen, M. P. (1987) in "*Computer Simulation of Liquids*", Clarendon Press.
[28] Maitland, G. C., Rigby, M., Smith, E. B. and Wakeham, N. A. (1981) in "*Intermolecular Forces*", Clarendon Press.
[29] Pellenq, R. J-M. and Nicholson, D. (1994) "Intermolecular potential function for the physical adsorption of rare gases in silicalite", *J. Phys. Chem.*, **98**, 13339.
[30] Nicholson, D., Boutin, A. and Pellenq, R. J-M. "Intermolecular potential functions for adsorption in zeolites: state of the art and effective models", *Mol. Sim.*, this issue.
[31] Claverie, P. (1978) in "Intermolecular interactions, from diatomics to biopolymers", Pullman ed, B. Wiley.

Downloaded At: 19:17 14 January 2011

[32] Stone, A. J. and Tong, C. S. (1995) "Anisotropic repulsion", *J. Comp. Chem.*, **15**, 1377.
[33] Böhm, H. J. and Ahlrichs, R. (1982) " A study of short range repulsions", *J. Chem. Phys.*, **77**, 2028.
[34] Tang, K. T. and Toennies, J. P. (1984) "An improved simple model for the van der Waals potential based on universal damping functions for the dispersion coefficients". *J. Chem. Phys.*, **80**, 3726.
[35] Pellenq, R. J-M. and Nicholson, D. (1995) "Grand ensemble Monte-Carlo simulation of simple molecules adsorbed in silicalite-1" *Langmuir*, **11**, 1626.
[36] Rees, L. V. C., Bruckner, P. and Hampson, J. (1991) "Sorption of N_2, CH_4 and CO_2 in silicalite-1", *Gas Sep. and Purif.*, **5**, 67.
[37] Boutin, A., Pellenq, R. J -M. and Nicholson, D. (1994) "Molecular simulation of the stepped adsorption isotherm of methane in $AlPO_4-5$", *Chem. Phys. Letters*, **219**, 484. Lachet, V., Boutin, A., Pellenq, R. J.-M. and Nicholson, D. Fuchs, A. H. (1996) "Molecular simulation of the structural rearrangement of methane adsorbed in aluminophosphate $AlPO_4-5$", *J. Phys. Chem.* in press.
[38] Pellenq, R. J- M., Tavitian, B. and Espinat, D., Fuchs, A. H. (1996) "Grand Monte-Carlo simulations of adsorption of polar and non-polar molecules in NaY zeolite", in press *Langmuir*. Pellenq, R. J- M., Fuchs, A. H. Institut Français du Pétrole, internal report, (1995).
[39] Fernandez-Alonso, F., Pellenq, R. J-M. and Nicholson, D. (1995) "The role of three-body interaction in the adsorption of argon in silicalite-1", *Mol. Phys*, **86**, 1021.
[40] Alejandre, J., Tildesley, D. J. and Chapela, G. A. "Molecular dynamics simulation of the orthobaric densities and surface tension of water (1995)", *J. Chem. Phys.*, **102**, 4574 and references therein.
[41] Jedlovszky, P. and Palinkas, G. (1994) "Monte-Carlo simulation of liquid acetone with a polarizable molecular model", *Mol. Phys.*, **84**, 217.
[42] Freeman, N. (1994) PhD thesis, University of London, Imperial College.
[43] Metropolis, N., Rosenbluth, A. W., Rosenbluth, M. N., Teller, A. H. and Teller, E. (1953) "Equation of state calculations on fast computing machines", *J. Chem. Phys.*, **21**, 1087.
[44] Tosi-Pellenq, N. J. M. (1994) PhD thesis, Université de Provence (Marseille).
[45] Watanabe, K. Austin, N. and Stapleton, M. R. (1995) "Investigation of the air separation properties of zeolites types A, X, and Y by Monte Carlo simulations", *Mol.Sim.*, **15**, 197.
[46] Fyfe, C. A., Kennedy, G. J., De Schutter, C. T. and Kokotailo, G. T. (1984) "Sorbate-induced structural changes in ZSM-5 (silicalite)", *J. Chem. Soc. Chem. Commun.*, 541.
[47] Dongfeng Pan Mersmann, A. B. (1991) "Methods for incorporating adsorbent activity into zeolitic adsorption isotherms", *Gas Sep. Purif.*, **5**, 210 (1991). Dongfeng Pan, Mersmann, A. B. "How can an adsorption system show phase transition", Characterization of Porous Solids II, F. Reinoso *et al.* eds., Studies in Surface Science and Catalysis, Elsevier, **62**, (1991).
[48] Muller, A. J. and Conner, W. C. (1993) "Cyclohexane in ZSM-5. FTIR and X-ray studies", *J. Phys. Chem.*, **97**, 1451.
[49] Janchen, J., Peeters, M. P. J., De Haan, J. W., van de ven, L. J. M., Van Hoof, J. H. C., Girmus, I. and Lohse, U. (1993) "Adsorption, calorimetric measurements and ^{27}Al DOR NMR studies on the molecular sieves $AlPO_4$-18", *J. Phys. Chem.*, **97**, 12042.
[50] Golden, T. C. and Sircar, S. (1994) "Gas adsorption on silicalite", *J. Coll. Int. Sci.*, **162**, 182.
[51] Baur, W. (1992) "Self-limiting distortion by antirotating hinges is the principle of flexible noncollapsible frameworks", *J. Solid State Chem.*, **97**, 243.
[52] Coulomb, J. P. (1993) private communication
[53] Parsonage, N. G. and Staveley, L. A. K. (1978) in "Disorder in crystals", Monographs on Chemistry, Rowlinson, J. S., Baldwin eds, J. E. (1978) Clarendon Press.
[54] Demontis, P., Suffritti, G. B., Quartieri, S., Gamba, A. and Fois, E. S. (1991) "Molecular dynamics studies on zeolites, discussion of the structural changes of silicalite", *J. Chem. Soc. Faraday Trans.*, **87**, 1657.
[55] Yamazaki, T., Watanuki, I., Ozawa, S. and Ogino, Y. (1988) "Infrared spectra of methane adsorbed by ion exchanged ZSM-5 zeolites", *Langmuir*, **4**, 433.
[56] Tosi-Pellenq, N. J. M., Llewellyn, P., Grillet, Y. and Rouquerol, J. (1992) "Microcalorimetric study of the adsorption of various gases into microporous adsorbents: a model aluminophosphate and a natural clay", *Therm. Acta*, **204**, 79.

Downloaded At: 19:17 14 January 2011